Hindawi
Journal of Nanomaterials
Volume 2019, Article ID 9641860, 16 pages
https://doi.org/10.1155/2019/9641860

Research Article

Artificial Sweeteners and Sugar Ingredients as Reducing Agent for Green Synthesis of Silver Nanoparticles

Shohreh Hemmati,[1,2] **Erin Retzlaff-Roberts**,[1] **Corren Scott**,[1] **and Michael T. Harris**[1]

[1]*Davidson School of Chemical Engineering, Purdue University, West Lafayette, IN 47907, USA*
[2]*School of Chemical Engineering, Oklahoma State University, Stillwater, OK 74078, USA*

Correspondence should be addressed to Michael T. Harris; mtharris@purdue.edu

Received 7 April 2018; Revised 29 August 2018; Accepted 10 September 2018; Published 21 January 2019

Academic Editor: Haisheng Qian

An environmentally friendly technique has been developed to produce metal nanoparticles using green synthesis methods. In this study, silver nanostructures were synthesized using different sugar substitutes and artificial sweeteners as green reducing agents in an aqueous solution at low temperature. The main ingredients (such as maltodextrin, sucrose, saccharin, and sucralose) of the artificial sweeteners acting as reducing agents were used to reduce Ag^+ ions to Ag^0. The pH of the solution was controlled during synthesis through the addition of sodium hydroxide (NaOH) to increase the strength of the reducing agents by converting nonreducing sugars to reducing ones and consequently increasing the rate of silver nanoparticle formation. The size and morphology of the synthesized nanostructures were characterized by transmission electron microscopy (TEM), high-resolution transmission electron microscopy (HRTEM), scanning electron microscopy (SEM), and energy-dispersive X-ray spectroscopy (EDX). The formation of nanostructures during the course of the reactions was investigated by UV-visible (UV-vis) spectroscopy characterization of an aliquot of sample at specific intervals. The function of each artificial sweetener and corresponding ingredients as a reducing agent and capping agent was investigated by Fourier-transform infrared spectroscopy (FTIR) and mass spectrometry (MS).

1. Introduction

Around fifty years ago, it was suggested that the material characteristics could be improved by miniaturization [1, 2]. Nanomaterials were used in ancient times with limited ability to probe at the nanoscale and limited understanding of nanotechnology [3, 4]. Based on the unique properties such as size, morphology, and high surface to volume ratio, nanoparticles show novel and improved characteristics [5, 6]. The synthesis of nanomaterials can be done by several chemical and physical methods including but not limited to microwave assisted, hydrothermal, heat evaporation, chemical reduction, photochemical reduction, electrochemical reduction, and so on. While nanomaterials can be successfully synthesized using these techniques, there are numerous drawbacks including high cost and the application of toxic solvents and external reducing agents, excessive material conversion, sophisticated equipment, and high-energy requirements [5, 7–15]. However, green synthesis approaches aim to achieve sustainable development of nanomaterials through the application of natural products such as reducing agents with inherent growth terminating, stabilizing, and capping characteristics [16, 17]. Moreover, the typical metal nanoparticle synthesis usually can easily incorporate contaminants that would cause further issues in a specific application [18]. Plant extracts or biological microorganisms in biosynthesis methods and also new energy transfer equipment have been utilized as simple, environmentally friendly, and viable alternative approaches to chemical and physical approaches that meet the green chemistry requirements [6, 19–21]. Utilizing different plant materials for nanoparticle synthesis is known as a green approach, since it does not involve any toxic or harmful chemicals [5, 20, 22–26].

Previous studies have focused on the importance of metal nanoparticles such as silver (Ag), palladium (Pd),

gold (Au), copper (Cu), and platinum (Pt) due to their unique physicochemical characteristics, nanoscale size, and surface plasmon behavior [5, 27–30]. Among these, silver nanoparticles (AgNPs) have unique and outstanding shape and size-dependent electrical, thermal, optical, catalytic, optoelectronic, anticancer, biosensing, medicinal, antiviral, and biological characteristics, which make them exceptional for several applications in a variety of fields and disciplines such as dentistry, drug delivery, biomedical, anticancer, antimicrobial, antioxidant, food science, agriculture, cosmetic, clothing, water treatment, larvicides, forensic science pollution control, waste management, photovoltaics, and chemistry [5, 10, 30–36].

Different functional groups in green reducing agents such as ketone, aldehyde, hydroxyl, amine, and carboxyl can be responsible for the reduction of different metal ions to metal atoms [37]. Understanding the functionality of each group in the reduction, nucleation, and growth of metal nanostructures would make it easier to predict the applicability of other novel green reducing agents for the metal nanostructure synthesis. Moreover, this investigation would be essential in understanding how the size and morphology of the synthesized nanostructures could be controlled. It has been reported that the *Stevia rebaudiana* leaves, as one of the zero-calorie sweetener plants, has potential for metal nanostructure synthesis [38]. The presence of aldehyde groups and its concentration in the reducing sugars play an essential role in nanoparticle formation [39]. Different types of reducing agents contain different types of sugars such as dextrose [40], monosaccharide and polysaccharide [39], honey [41], dextrose and maltose [23], and D-glucose [42] that have been utilized for the synthesis of silver nanostructures. Some of these reducing agents such as glucose [43] and different types of sugars [42, 44] have been utilized in the presence of ammonia or sodium hydroxide as accelerator reagents to control the pH and increase the rate of the reduction and growth of silver nanoparticles.

There are several sugar substitutes and artificial sweeteners that can be made in the laboratory such as sucralose, saccharin, and aspartame or can be natural products such as xylitol and sorbitol. There are different commercially available sugars (white and brown sugar), sugar substitutes, and artificial sweeteners named in different brands: Splenda, Sweet'n Low, Equal Original, Caribou Coffee, Great Value, Stevia Blend, Whole Earth, NJOY, and so on. As each of those consists of the combination of different ingredients such as saccharin, aspartame, neotame, acesulfame potassium, sucralose, cyclamate, sorbitol, xylitol, erythritol, and steviol, with different functional groups such as NH-, OH-, NH_2-, OCH_3-, and CH_2OH-, they can be used as green and sustainable reducing agents for the reduction of metal ions. The ability of each artificial sweetener as a reducing and stabilizing agent in metal nanostructure synthesis strongly depends on its ingredient and its corresponding functional groups. Figure 1 shows an example of the different main ingredients of some artificial sweeteners and their chemical structures. The color of their packets is based on their ingredients, specifically their sweetening component. For instance, brown sugar is a sucrose-based sugar with an intense brown color because of the presence of molasses or black treacle. Splenda is a sucralose-based artificial sweetener, containing about 95 vol.% dextrose (D-glucose) and maltodextrin, combined with a small amount of sucralose. Sweet'n Low is a brand of artificial sweetener made primarily from granulated saccharin that also contains dextrose and cream of tartar.

2. Experimental

2.1. Material. All of the reagents and materials such as silver nitrate ($AgNO_3$, Sigma-Aldrich, 10220, 99.8–100.5%), poly(vinyl pyrrolidone) (PVP, Sigma-Aldrich, 856568, Avg. MW: 55000), sucrose (ChemSupply, D(+) sucrose for biochemistry 99.7%), sucralose (Sigma-Aldrich, PHR1342), saccharin (Sigma-Aldrich, 240931), maltodextrin (Sigma-Aldrich, 41967, dextrose equivalent 4.0–7.0), acetone (PHARNCO-AAPER, C14E15003), sodium hydroxide (Fisher Scientific, SS255-1, 10 N solution, 30% *w*/*w*), and distillated water (DIW) were used as received.

2.2. Silver Nanoparticle Synthesis. An aqueous solution of 2 wt.% of each sugar or sweetener in a glass flask (around 30 mL reaction solution in 100 mL flask) was heated at 50°C for 15 min under continuous magnetic stirring. After 15 min preheating, reagent solutions of 1 or 10 mM silver nitrate were added slowly. The color of the reaction mixture changed from colorless to yellow and then to orange-brownish or green-grayish (depending on the size and morphology of the synthesized silver nanostructures) within 2 hours of the reaction time. To investigate the effect of temperature, the $AgNO_3$ solutions were added slowly to the beaker, containing 2 wt.% of each sugar or sweetener under magnetic stirring at room temperature (around 25°C) as well. In order to investigate the effect of poly(vinyl pyrrolidone) (PVP) as a capping agent for each reaction, different concentrations of PVP were added before adding the $AgNO_3$ solution. Moreover, at specific intervals (right after the solution injection and every 30 minutes) during the reactions, a specific amount of aliquot was taken out to do the UV-vis characterization. After nanoparticle formation, the reaction flask was cooled to room temperature. The solution was centrifuged at 3000 rpm for 60 min, and the supernatant was saved for further FTIR and mass spectrometry characterization. The particles were resuspended in DIW in the absence of PVP and in acetone in the presence of PVP and centrifuged at 3000 rpm for another 60 min. The centrifugation and separation were repeated two more times with the addition of DIW, and the product was then stored in DIW.

2.3. Characterization. Synthesized AgNPs were characterized by transmission electron microscopy (TEM), high-resolution transmission electron microscopy (HRTEM), scanning electron microscopy (SEM), energy-dispersive X-ray spectroscopy (EDX), and UV-visible (UV-vis) spectroscopy.

TEM images were taken using a 200 kV Tecnai T20 transmission electron microscope. Samples were prepared by depositing a 3 μL drop of AgNP suspension onto carbon formvar copper grids.

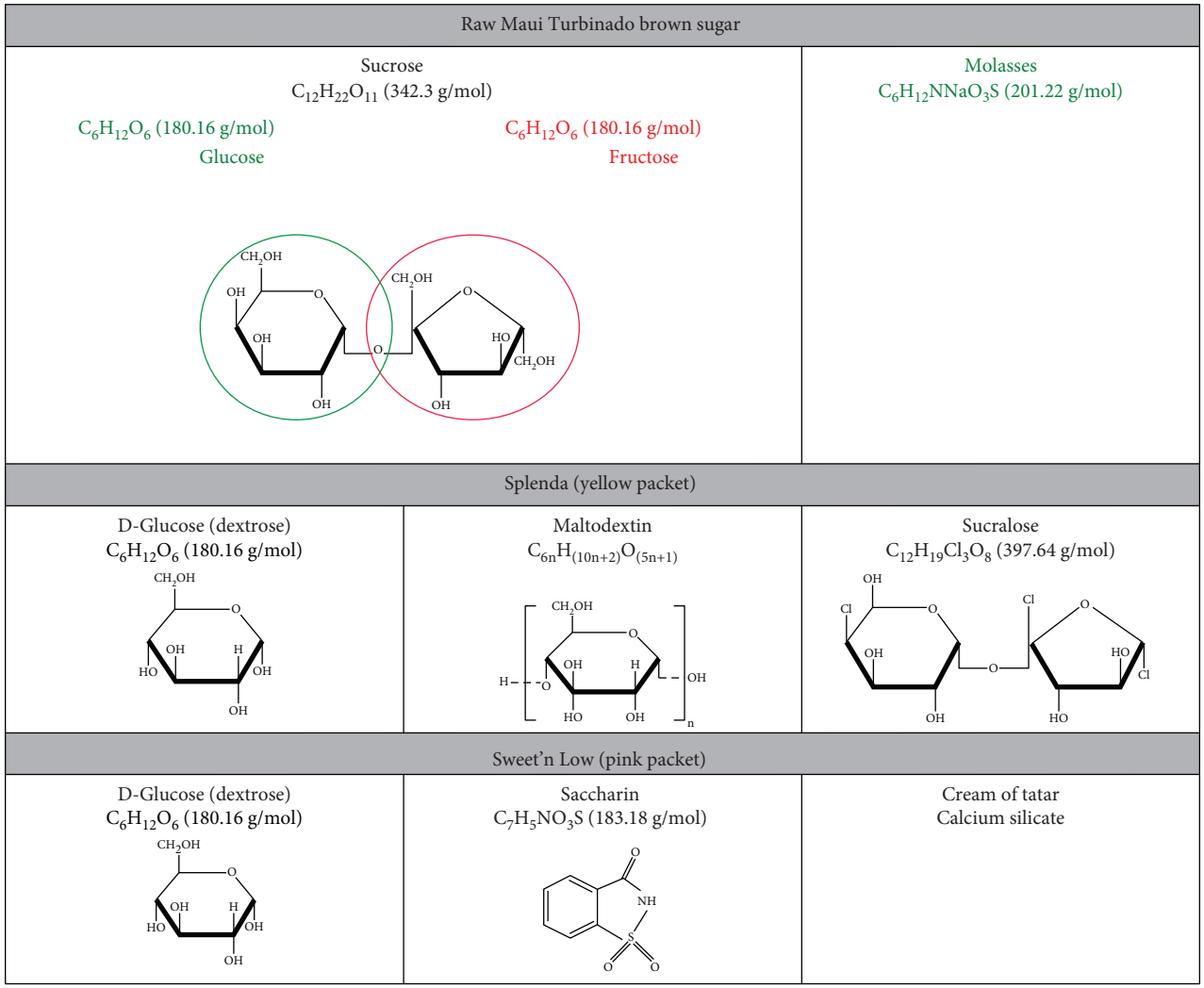

Figure 1: Main ingredients of some artificial sweeteners and sugar substitutes and their chemical structures.

For SEM (FEI NOVA nanoSEM Field Emission SEM), a drop of each sample was placed on a piece of cover glass, dried, and sputter-coated with Gold/Palladium (Au/Pd). SEM images were acquired with an FEI field emission microscope operating at an accelerating voltage of 7 kV.

The UV-vis spectra were taken by the Varian Cary 100 spectrometer. The UV-vis characterizations during the reaction were also used to investigate the kinetics of the reaction to see if there is increasing color intensity in the wavelength region of 200–800 nm with increasing time to monitor metal nanoparticle production.

FTIR and mass spectrometry characterizations were first done on each aqueous sugar or sweetener solution. The supernatant, after centrifugation and separation of the reacted solution, was saved for FTIR and mass spectrometry characterization. Vibrational spectroscopy characterizations of aqueous solutions are challenging due to the strong absorption of infrared radiation by water, the solvent, in wavenumber ranges, such as below 900, from 1400–2500, and above 3000 cm^{-1}. Attenuated total reflection (ATR) infrared accessories are the best alternatives to characterize aqueous solution. In this study, the Fourier-transform infrared spectroscopy was done using an ATR-FTIR accessory.

Same characterizations of the reducing agents before and after reduction were done using mass spectrometry (4800 Plus MALDI TOF/TOF (Applied Biosystems/MDS SCIEX)). The MS and MS/MS data were obtained in the positive mode, and the sample was prepared by adding 1 μL of sample in water to 1 μL of matrix, which was 10 mg/mL of 2,5-dihydroxybenzoic acid in 75% ethanol/water.

3. Results and Discussion

3.1. UV-vis Characterization during the Course of Reactions. By understanding the reaction mechanism, it is possible to know how the size and morphology of nanostructures can be controlled and tuned. The nanoparticle size and their quantitative formation can be studied and monitored by UV-vis absorption spectroscopy. The UV-vis characterization during the reaction can also be used to investigate the kinetics of the reaction. For instance, in most green synthesis processes of metal nanostructures, their formation and

growth are slow in the beginning of the reaction but are accelerated as soon as the initial seeds form that correspond to the sigmoidal kinetic [45, 46]. AgNPs adsorb radiation in the range of 380–450 nm, corresponding to the visible range of electromagnetic spectrum because of the surface plasmon resonance (SPR) transition due to the yellowish-brownish color. The maximum UV-vis absorption at 400–430 nm for 2–20 nm AgNPs was reported in previous studies [47–51]. Moreover, different studies have shown that Ag clusters illustrate different optical spectra based on the number of Ag atoms in that cluster. Ag^0 produced in the course of metal ion reduction may undergo some transformation through cluster formation. For instance, the optical band corresponding to Ag_8^{2+} in the absorption spectrum differs from the bands typical for Ag (360 nm) and Ag^{2+} (310 nm) dimers and disappears as Ag_8^{2+} cluster transforms in a silver sol [52].

Figure 2 shows the UV-vis characterization during the AgNP synthesis utilizing different artificial sweeteners and sugar substitutes at 50°C. This figure shows an increase in peak size in the SPR spectra region. Thus, more reduction is observed that illustrates and quantifies the reduction process over time. Application of some of the artificial sweeteners such as Caribou Zero Calories, Sweet'n Low, and Equal Original did not cause any peak in the desired range corresponding to the formation of AgNPs during the course of the reaction. On the other hand, Splenda, Maui Raws Turbinado sugar (brown sugar), and white sugar showed a broad peak in the area of 400–550 nm indicating the formation of AgNPs. The color change of the reaction solution primarily indicated the AgNP formation. These color changes were due to the reduction of Ag^+ ions to Ag^0 atoms and formation of AgNPs of different sizes. The observed broad peaks can be due to the large size distribution of the synthesized AgNPs. Broader SPR peaks at the beginning of the reactions indicate the broad size distribution in the early stages of the reactions that become smaller as the reactions continue with narrower SPR peaks. The spectrum also shows the increment in intensity that is due to the continuous reduction of Ag^+ ions and increasing formation of AgNPs. Sometimes, decreasing of absorption values and shifting to longer wavelength are an indication of aggregation as the synthesis processes continue. As temperature is one the most important parameters in metal nanoparticle synthesis, the reactions were repeated at a lower temperature of 25°C (Figure S1). In traditional chemical AgNP synthesis, high temperature (above 150°C) is required at the very beginning of the reaction to convert reducing agent and, consequently, the reduction of silver ions to silver atoms. The result of this study shows that the reduction of silver ions to silver atoms can be done at low temperature (as low as 25°C) in green methods utilizing sugar substitutes as a reducing agent. A higher temperature of 50°C can increase the ability of sugars as reducing agents in the reduction of silver ions and formation of silver nanoparticles.

Another essential parameter in the synthesis of metal nanoparticles is the metal precursor concentration and its ratio to the reducing agent. Figure 3 shows the UV-vis characterization during the AgNP synthesis utilizing Maui Raws Turbinado sugar (brown sugar) and Splenda at 50°C and a higher concentration of $AgNO_3$ at 10 mM, while the reducing agent concentration is constant. The color of the final reaction solution (silver nanostructure suspension) that depends on the size and morphology of the synthesized silver nanostructures is also shown in this picture. In the case of brown sugar as a reducing agent, the color is green-grayish, which indicates the presence of one-dimensional (1D) silver nanostructures. On the other hand, in the case of Splenda as a reducing agent, the orange-brownish color is an indication of silver nanosphere or nanocubes.

It should be mentioned that in the AgNP synthesis, the concentration of $AgNO_3$ has a strong effect on the morphology and yield of the synthesized silver nanostructures. It is necessary to provide a low concentration of silver seeds at the beginning of the reaction, as well. To achieve this goal, the $AgNO_3$ solution was added slowly and dropwise in all of the synthesis processes. Moreover, as the preparation of $AgNO_3$ solution may have an effect on the morphology and yield of the synthesized AgNPs, the aqueous solution of $AgNO_3$ was sonicated for approximately 2–3 minutes.

When the $AgNO_3$ concentration as a metal precursor is low, it is not able to provide enough silver ions for seed nucleation. While its concentration is increasing, the yield of synthesized AgNPs increases but up to a limit. More studies are required to find this limit based on reaction optimization through the design of experiment (DoE).

As mentioned before, the packet's color of each artificial sweetener is based on its main ingredient. The Splenda in the yellow packet tended to yield a higher intensity in the SPR spectra, indicating a stronger ability as a reducing agent in comparison to the other artificial sweeteners in the yellow packet, such as Equal Original, NJOY, and Great Value.

Figure 4 illustrates the UV-vis characterization during the AgNP synthesis utilizing Splenda, Equal Original, NJOY, and Great Value in the yellow packet as reducing agents at 50°C and 10 mM $AgNO_3$ concentration. It is clear that the main ingredients strongly affect the AgNP formation, as there is no AgNP formation for the Equal Original in the pink packet, while the UV-vis spectra show the formation of AgNPs with the yellow one at the same reaction conditions.

PVP plays an essential role, acting as a stabilizer, in controlling the growth and elongation of the initially formed silver seeds to the wire shape in polyol (one of the conventional chemical synthesis methods) synthesis of silver nanowires (AgNWs). Both concentration and molecular weight (MW) of PVP are essential to control the morphology of the synthesized AgNWs [53, 54]. PVP was utilized as a capping agent in the green AgNP synthesis to investigate the possibility of the control of the initially formed Ag seeds to one-dimensional (1D) nanostructures in green synthesis. PVP is a versatile polymer for biomedical applications due to its biocompatibility that comes from the absence of toxicity to form its complexes [55]. Even though PVP is not obtained from a green chemical route, it is necessary to find out if it can have the same effect as in traditional

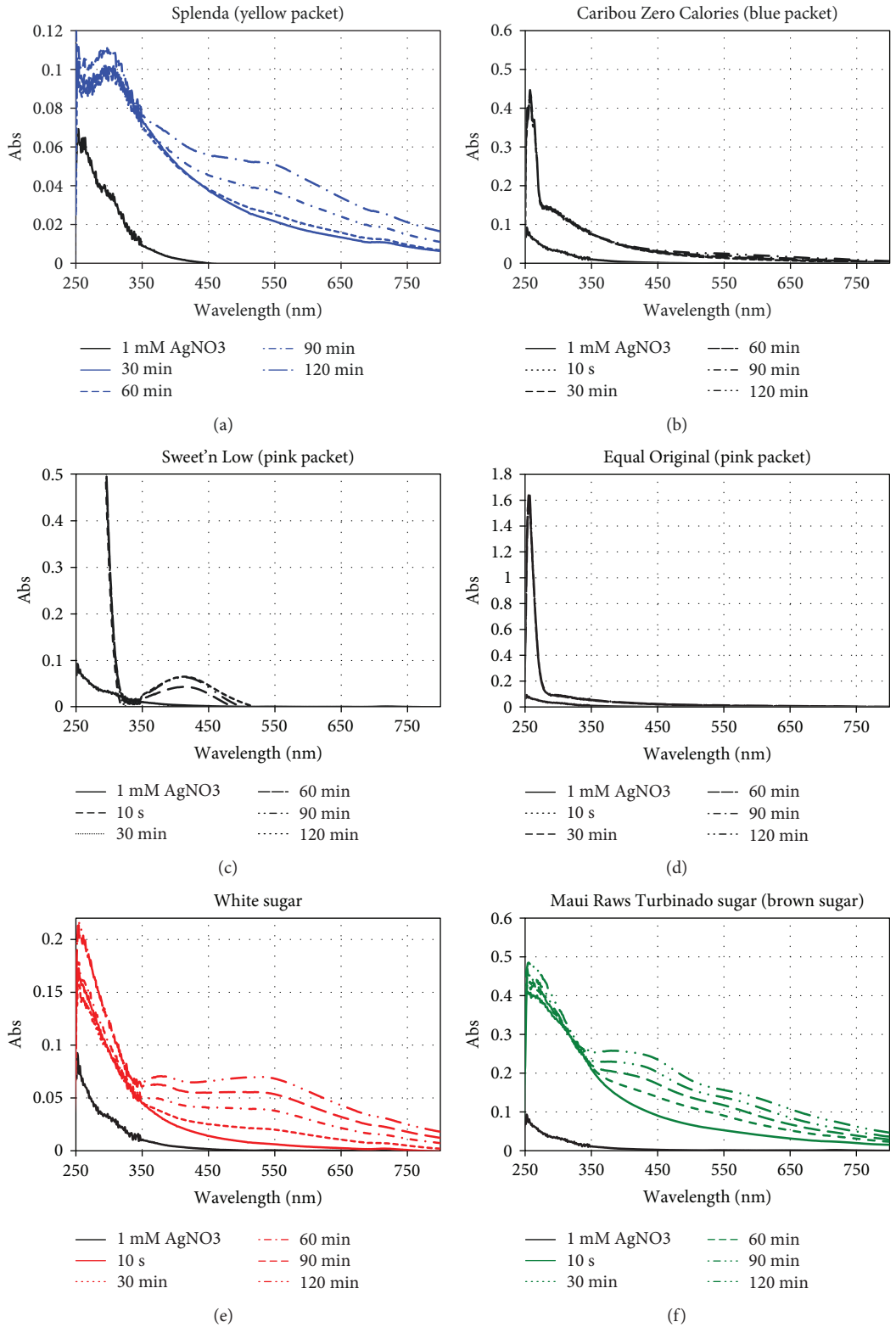

Figure 2: UV-vis characterization during the synthesis of AgNPs (1 mM $AgNO_3$, 2 wt.% sugar substitutes or artificial sweeteners, $T = 50^{\circ}C$, 2 h reaction time).

methods such as the polyol synthesis method. This finding will be essential in finding other green capping agents that can act as a capping agent in the synthesis of 1D silver nanoparticles in the same manner as PVP by selective adsorption on the {100} facets of the initially formed silver seeds through Ag-O bonding. Figure S2 illustrates the UV-vis characterization during the AgNP synthesis utilizing Maui Raws Turbinado sugar (brown sugar) and Splenda at 50°C

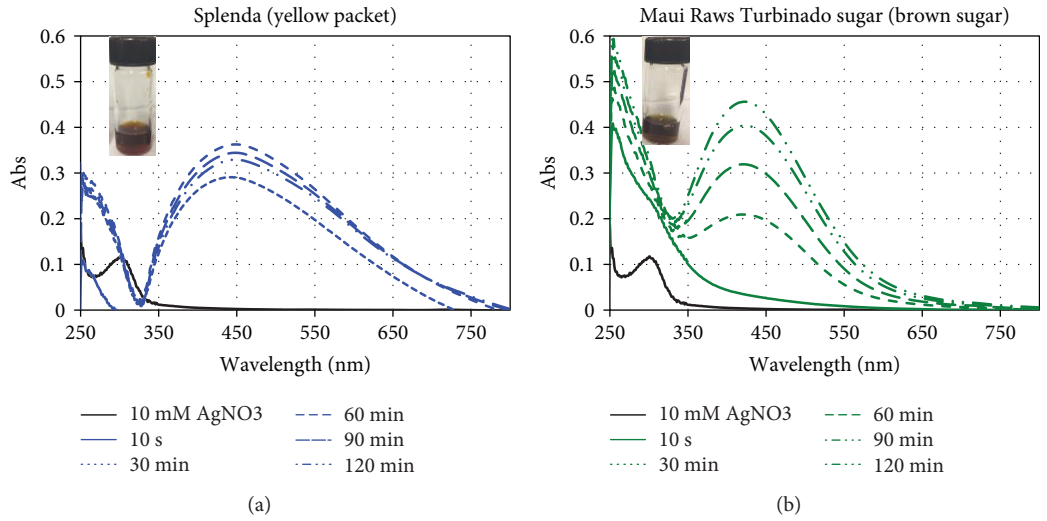

Figure 3: UV-vis characterization during the synthesis of AgNPs (10 mM $AgNO_3$, 2 wt.% sugar substitutes or artificial sweetener, $T = 50^{\circ}C$, 2 h reaction time).

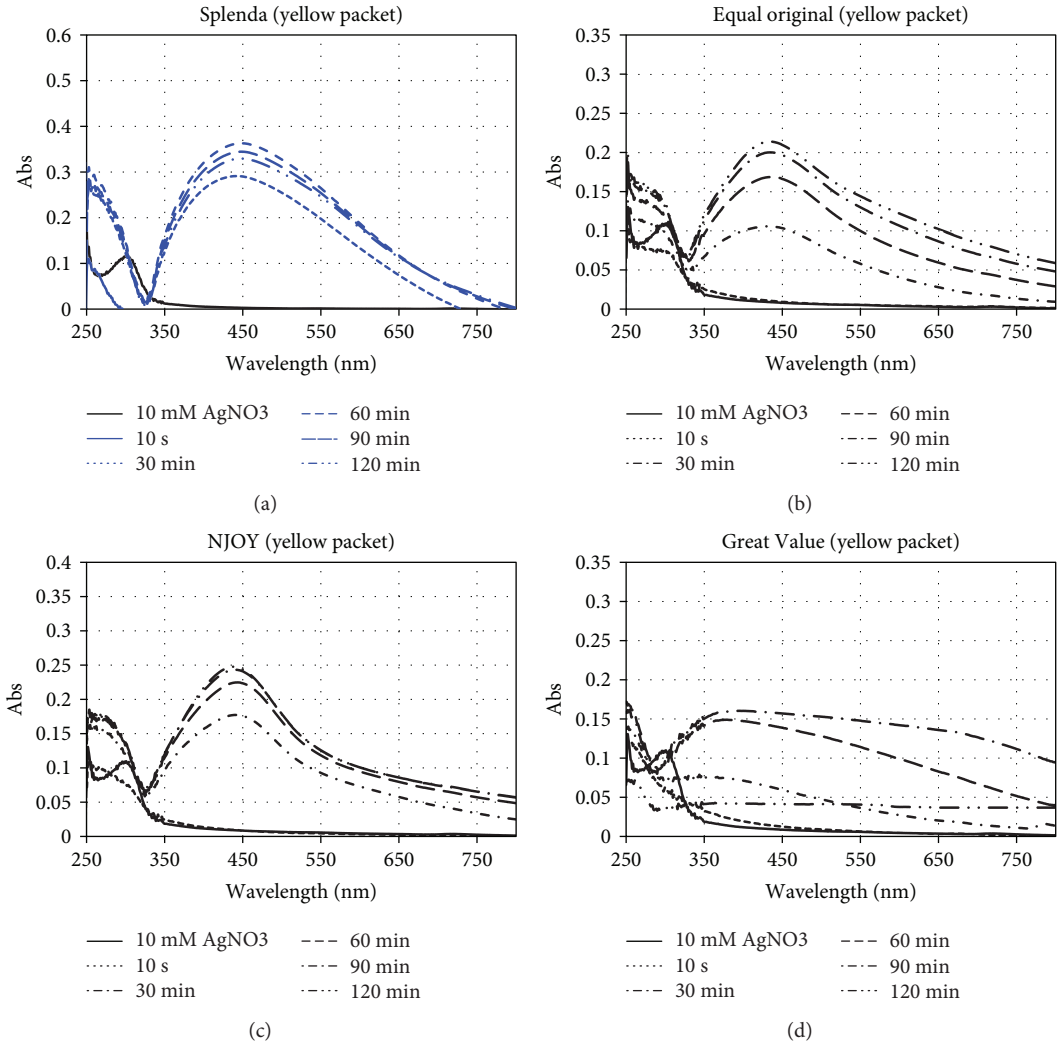

Figure 4: UV-vis characterization during the synthesis of AgNPs (10 mM $AgNO_3$, 2 wt.% sugar substitutes or artificial sweeteners, $T = 50^{\circ}C$, 2 h reaction time).

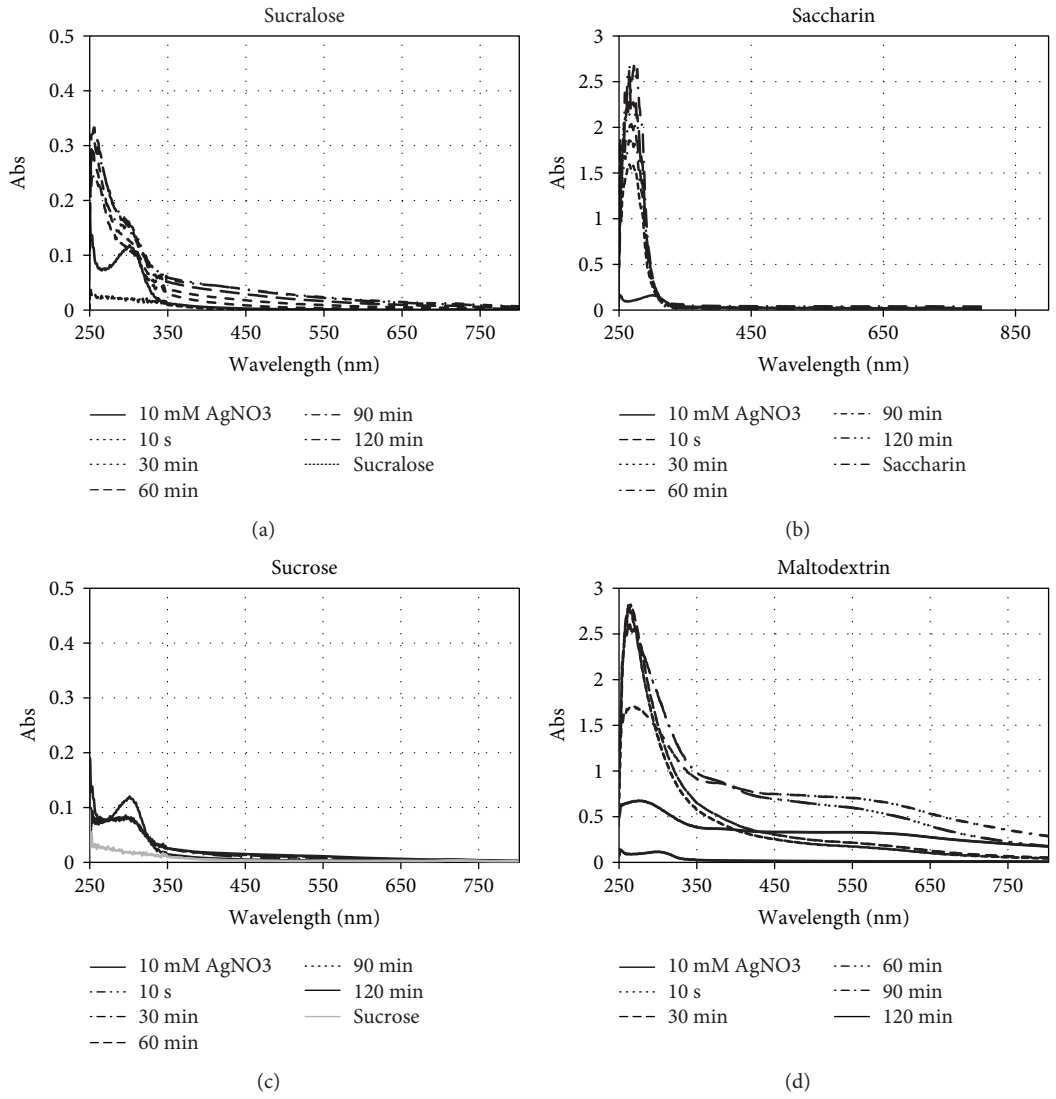

Figure 5: UV-vis characterization during the synthesis of AgNPs (10 mM $AgNO_3$, $T = 50^{\circ}C$, 2 h reaction time).

in the presence of PVP as a capping agent. This figure illustrates how the PVP affects the UV-vis spectra by narrowing the peaks in the case of brown sugar and increasing absorbance in the case of Splenda as the reducing agent. Normally, the sharp peaks around 350 and 390 nm correspond to the transversal surface plasmon resonance (SPR) modes of AgNWs, and the absence of the peaks at more than 400 nm corresponding to AgNPs demonstrates the purity of the AgNWs. Based on this figure, there should be mostly AgNPs rather than 1D structures [56]. Even though the peaks in the desired region confirmed the formation of AgNPs, the size and morphology should further be investigated through TEM and HRTEM characterization. All of the other sweeteners in the yellow packet studied in this work were also tried in the presence of PVP as the capping agent. Figure S3 illustrates the UV-vis characterization during the AgNP synthesis utilizing Splenda, Equal Original, NJOY, and Great Value in the yellow packet as reducing agents at $50^{\circ}C$, 10 mM $AgNO_3$ concentration, and 16 mM PVP concentration. The comparison between Figure 4 and Figure S3 illustrates how the PVP affect the UV-vis spectra by increasing the absorbance in the case of Equal Original and NJOY as reducing agents or by narrowing the peaks in the case of Great Value as a reducing agent. It seems that the utilization of Splenda as a reducing agent in the presence of PVP as the capping agent caused less reduction of silver ions and formation of silver nanoparticles compared to the Splenda without PVP. It can be due to the fact that the concentration of ingredient acting as the reducing agent in Splenda is too high compared to the other reducing agents in the yellow packets. By considering the fact that PVP can also act as the reducing agent, maybe the concentration of reducing agent is too high compared to the Ag precursor concentration.

Based on these UV-vis characterization results, it is clear that the AgNPs can be synthesized by utilizing the artificial sweeteners and sugar ingredients in the yellow packets. Based on Figure 1, the ingredients of these sweeteners are dextrose, maltodextrin, and sucralose, and the main ingredients of the

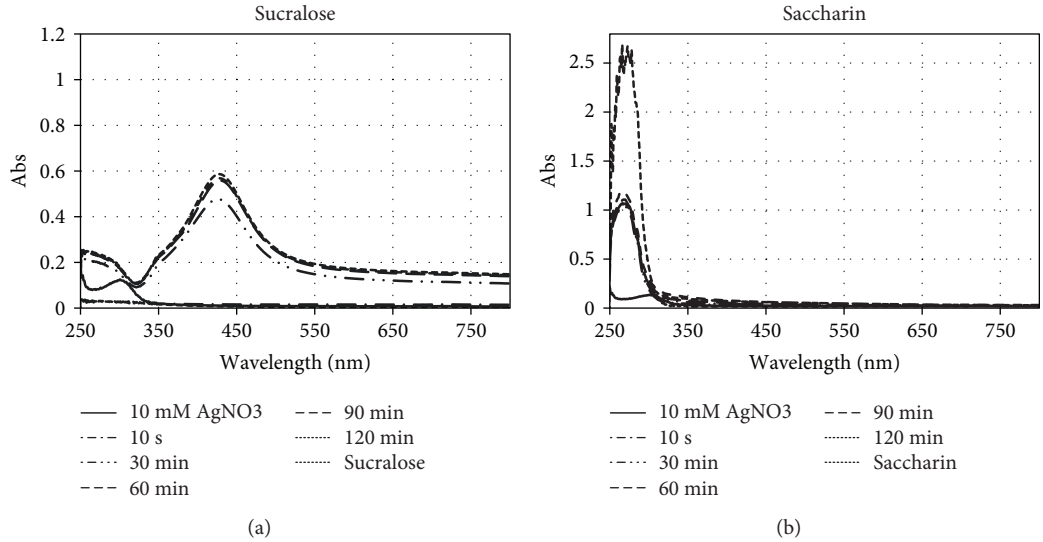

Figure 6: UV-vis characterization during the synthesis of AgNPs in the presence of NaOH (10 mM $AgNO_3$, $T = 50^{\circ}C$, 2 h reaction time).

sweeteners in the pink packet are dextrose and saccharin that could not act as reducing agents in AgNP synthesis. These main ingredients were utilized as reducing agents at the same reaction conditions as those corresponding sweeteners. Sucralose was used in the same concentration as corresponding sweetener (2 wt.%), but as the water solubility of saccharin is much less than 2 wt.% (1 g/290 mL), it was used at a lower concentration to prevent supersaturation. Figure S4 and Figure 5 show the UV-vis characterization during the AgNP synthesis utilizing sucralose, saccharin, sucrose, and maltodextrin as reducing agents for 1 mM and 10 mM $AgNO_3$, respectively. Based on these UV-vis results, sucrose, sucralose, and saccharin could not act as reducing agents at those reaction conditions, but maltodextrin could act as a reducing agent.

When sugars are acting as reducing agents, it is essential to utilize the reducing sugars versus non-reducing sugars. Either these main ingredients are nonreducing sugars, or they cannot be converted to reducing sugars under the reaction conditions. A reducing sugar is any sugar that can act as a reducing agent containing either free aldehyde or free ketone groups. For instance, all simple sugars (monosaccharide) are reducing sugars, while sucrose (table sugar) and maltose are nonreducing ones. Reducing sugars under heating and alkaline environment are usually oxidized into gluconate and other products that can act as reducing agents [49]. As it has been reported, alkaline hydrolysis of nonreducing sugars such as sucrose (white sugar) can release reducing sugars such as glucose and fructose that can be responsible for the reduction of Ag^+ ions to Ag^0 atoms. Moreover, the rate of AgNP synthesis can be strongly affected by pH and the quantities of alkaline solution utilized in the synthesis processes [44]. To investigate the pH effect, the main ingredients of artificial sweeteners (saccharin and sucralose that could not act as reducing agents at that reaction condition) were utilized in the presence of NaOH, and the pH was recorded every two minutes during the reaction. Figure 6 illustrates the effect of NaOH addition in

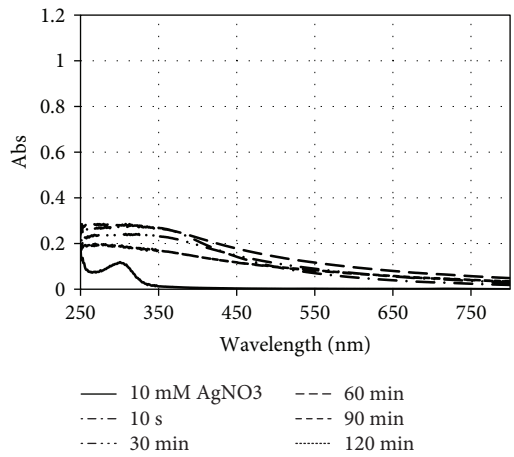

Figure 7: UV-vis characterization during the synthesis of AgNPs utilizing NaOH as a reducing agent (10 mM $AgNO_3$, $T = 50^{\circ}C$, 2 h reaction time).

the synthesis of AgNPs utilizing saccharin and sucralose as reducing agents. In the case of saccharin as the reducing agent, the color of the reaction solution changed to yellow and then slightly brownish-yellow within the first 1 minute in the presence of NaOH. In the case of sucralose, the reaction solution color changed to a dark, dense brown-olive color within the first 1 minute. Due to the dense color of the reaction solution, the aliquots were diluted by a factor of 10 for UV-vis characterization. Finally, in order to investigate how NaOH can be utilized as a reducing agent, the synthesis was repeated without the addition of any external reducing agent as shown in Figure 7. The pH change during the synthesis is shown in Figure S5 for saccharin and sucralose as the reducing agents in the presence of NaOH and in Figure S6 for NaOH as the reducing agent. It is clear that the temporal variation of pH is different for these three reducing agents. The average of pH during the preheating

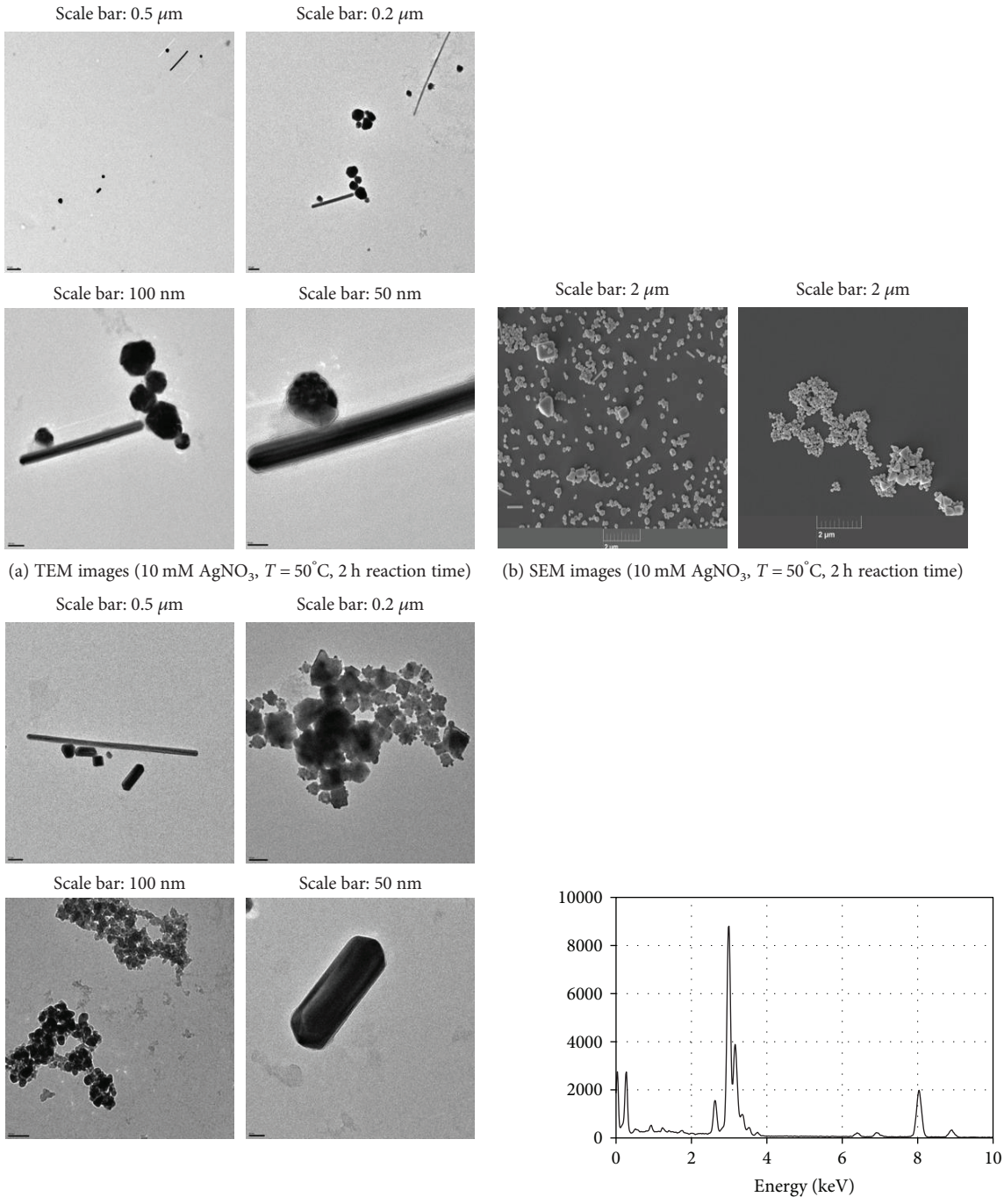

(a) TEM images (10 mM $AgNO_3$, $T = 50^{\circ}C$, 2 h reaction time)

(b) SEM images (10 mM $AgNO_3$, $T = 50^{\circ}C$, 2 h reaction time)

(c) TEM images (10 mM $AgNO_3$, 16 mM PVP, $T = 50^{\circ}C$, 2 h reaction time)

(d) EDX analysis (10 mM $AgNO_3$, $T = 50^{\circ}C$, 2 h reaction time)

Figure 8: TEM, SEM, and EDX characterization of the synthesized ANPs utilizing brown sugar as a reducing agent.

for 15 minutes was 10.57, 6.97, and 1.62 for NaOH, sucralose, and saccharin, respectively. Right after the addition of NaOH as the pH controller, in the cases of sucralose and saccharin as reducing agents, the pH reached 10.83 for sucralose after the addition of 10 μL of NaOH, while for saccharin it reached 10.5 after the addition of 40 μL of NaOH. The average of the pH during the reaction was 11.16, 7.95, and 9.59 for NaOH, sucralose, and saccharin, respectively. These results are an indication regarding the strong effect of pH during the green synthesis of AgNPs on their size, yield, and morphologies. It showed that how the oxidation potential of sucralose and saccharin as reducing agents depends on pH. These can be further investigated by TEM characterization of the synthesized AgNPs. It should be also noted that it is not just the pH that gives the higher reduction. The suitable sweetener containing appropriate functional groups capable of acting as the reducing agents or convertible to reducing ones should be selected. For instance, maltose and sucrose that were used as reducing agents for AgNP synthesis have the same chemical formula

$C_{12}H_{22}O_{11}$ but different structures which could affect their reducing and capping ability. Maltose is a disaccharide and consists of two α-glucose units connected by a α-glycosidic bond that is a covalent bond between two monosaccharides that involves the carbon C_1 (anomeric) of the first unit of glucose and carbon C_4 of the second unit of glucose. Sucrose is a disaccharide consisting of one unit of α-glucose and one unit of β-fructose connected by β-glycosidic bond that is a covalent bond between two monosaccharides that involves carbon C_2 of the fructose and carbon C_1 (anomeric) of the glucose. Sucrose compared to maltose illustrates smaller interaction strength with water, higher partial molar volume, and smaller hydrogen bond. So sucrose has lower packed conformational arrangement than maltose, especially at the lower temperatures [57]. These results indicate that a further study is required to investigate the reduction ability of other sweeteners in other color packets such as pink (Sweet'n Low and Equal Original) in the presence of NaOH.

For more information, a summary of all of the UV-vis results is shown in Table S1 in terms of corresponding reaction conditions and UV-vis peak range.

3.2. Morphology of the Synthesized AgNPs. After confirming the production of AgNPs during the reaction, it is essential to characterize their morphology and size to see how different reducing agents and different reaction conditions can affect the morphology and yield of the synthesized AgNPs. The AgNPs synthesized through utilizing the Maui Raws Turbinado brown sugar and Splenda (yellow packet) in the presence and absence of PVP with the highest peaks in the UV-vis characterization during the reaction were used for TEM characterization. Figure S7 shows the TEM and HRTEM images of the synthesized AgNPs utilizing Maui Raws Turbinado brown sugar as the reducing agent and 1 mM $AgNO_3$ as the metal precursor. Figure 8(a) illustrates the TEM images of the synthesized AgNPs utilizing Maui Raws Turbinado brown sugar as the reducing agent and 10 mM $AgNO_3$ as the metal precursor. Figure 8(b) shows the corresponding SEM images. Figure 8(c) shows the same results in the presence of PVP as the capping agent.

When brown sugar was used as a reducing agent, it caused the elongation of the initially formed silver seeds to the 1D silver nanostructures such as nanorods and nanowires. This is the desired function of PVP as a capping agent to preferentially adsorb on {100} facets of the initially formed silver seeds, allow the addition of more Ag atoms to {111} facets, and consequently facilitate their growth to the 1D nanostructures. More interestingly, this specific brown sugar acted as both a reducing and a capping agent without the addition of PVP to synthesize 1D Ag nanostructures. Energy-dispersive X-ray spectroscopy (EDX) (Figure 8(d)) shows that these are constituted only of silver atoms (2.98 keV [Ag (Lα)] and 3.15 keV [Ag (Lβ)]).

Figures 9(a) and 9(b) show the TEM and the SEM images, respectively, of the synthesized AgNPs utilizing Splenda as the reducing agent with 10 mM $AgNO_3$ as the metal precursor. Figure 9(c) shows the TEM images of the synthesized AgNPs utilizing Splenda as the reducing agent with 10 mM $AgNO_3$ as the metal precursor and 16 mM PVP as the capping agent. The TEM and SEM images show that the type of a reducing agent has a strong effect on the morphology, size, and yield of the synthesized Ag

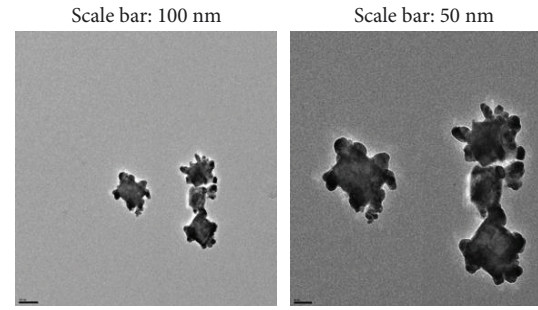

(a) TEM images (10 mM $AgNO_3$, $T = 50^{\circ}C$, 2 h reaction time)

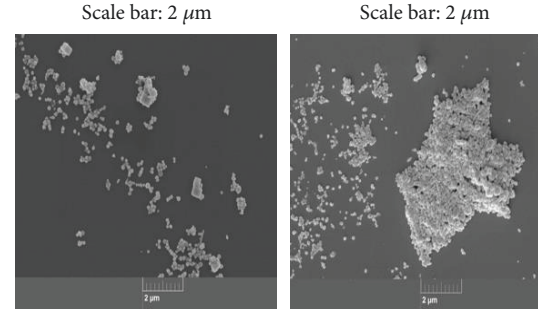

(b) SEM images (10 mM $AgNO_3$, $T = 50^{\circ}C$, 2 h reaction time)

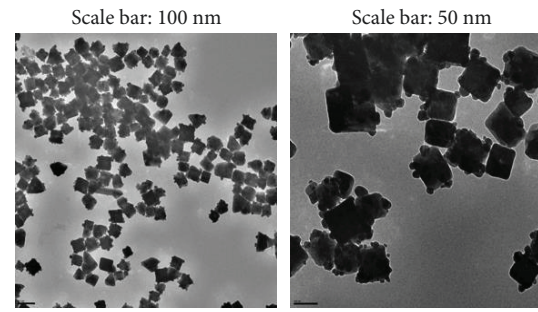

(c) TEM images (10 mM $AgNO_3$, 16 mM PVP, $T = 50^{\circ}C$, 2 h reaction time)

Figure 9: TEM and SEM images of the synthesized AgNPs utilizing Splenda (yellow packet) as a reducing agent.

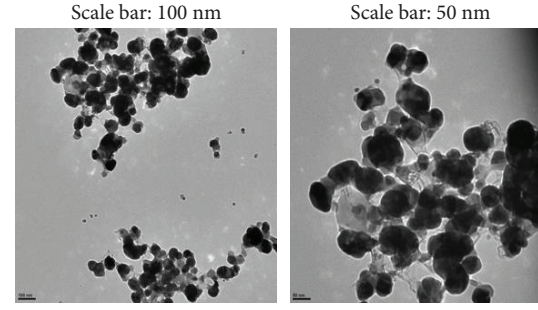

Figure 10: TEM images of the synthesized AgNPs utilizing maltodextrin as a reducing agent (10 mM $AgNO_3$, $T = 50^{\circ}C$, 2 h reaction time).

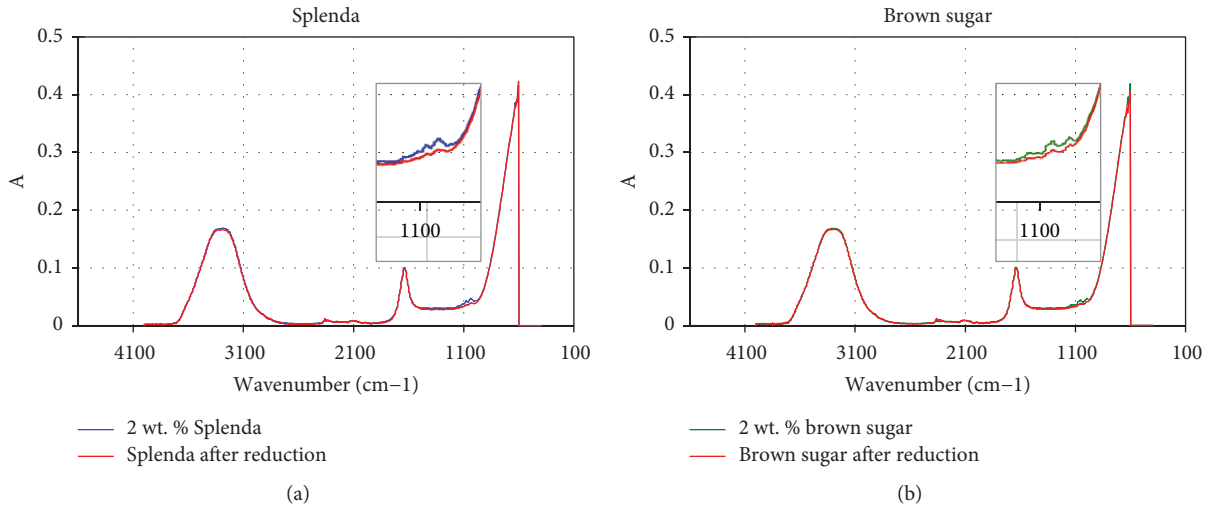

Figure 11: FTIR spectra of the reducing agents before and after Ag ion reduction (10 mM $AgNO_3$, $T = 50^{\circ}C$, 2 h reaction time). Inset pictures are the zoomed in spectra in regions corresponding to sugars.

nanostructures. PVP acted as a capping agent differently for brown sugar and Splenda. By utilizing Splenda as a reducing agent, PVP caused the formation of some small nanospheres as well as larger silver nanocubes. That can be due to the distribution adsorption of PVP on all facets of the initially formed silver seeds rather than selective adsorption on {100} facets.

Figure 10 illustrates the TEM images of the synthesized AgNPs utilizing maltodextrin as the reducing agent and 10 mM $AgNO_3$ as the metal precursor. Finally, the morphology of the synthesized AgNPs utilizing sucralose and saccharin as reducing agents in the presence of NaOH is shown in Figures S9(a) and S9(b), respectively.

3.3. FTIR Characterization of Reducing Agent before and after Reduction. Fourier transfer infrared spectroscopy (FTIR) is helpful to investigate the presence of the different functional groups from the position of the peaks in the spectrum [35, 39]. From the FTIR analysis, it is also possible to understand not only if the synthesized nanoparticles are surrounded by some metabolites or proteins such as amine, ketone, alcohol, aldehyde, carboxylate, or other functional groups but also if the stabilization of the systems results from functional groups of the reducing agents [58, 59]. In most cases, the water-soluble fractions in the green reducing agents play a complicated role in metal ion bioreduction and corresponding shape evolution of the metal nanoparticles that can be investigated by FTIR [46, 60]. This technique can also be used to see if the bioreductants can act as both a reducing agent and a capping ligand to stabilize metal nanoparticles in the solvent or not [61].

To find out which functional groups in a specific sweetener or its corresponding ingredients are responsible for the reduction of Ag ions or stabilizing its nanoparticles, the FTIR characterizations were done on Splenda (yellow packet) and Maui Raws Turbinado brown sugar as reducing agents before and after the reaction.

FTIR characterizations were done on their aqueous solution before reduction and after the reduction of the metal precursor. The FTIR characterizations before and after the reduction were compared to determine which functional groups were involved in the reduction of the metal precursor ions. These results are shown for Splenda (yellow packet) and Maui Raws Turbinado brown sugar in Figure 11. Some peaks were observed in the reducing agent spectra that disappeared in the spectra of the reducing agent after the reduction of the metal precursor ions. As the reducing agent solutions are too diluted (about 2 wt.%), it is hard to see the peaks sharply in the spectra, and the results are summarized in Tables 1 and 2 for brown sugar and Splenda, respectively, before and after reduction. Usually, reducing sugars illustrate ATR-FTIR peaks in the range of 850–1500 cm^{-1}, which can be the confirmation from sucrose, glucose, and fructose and characteristics of saccharide configurations. In this region, the 1500–1200 cm^{-1} can correspond to the deformation of $-CH_2$ and angular deformation of C-C-H and H-C-O, and the 1200–950 cm^{-1} region corresponds to the stretching mode of C-C and C-O. Although their bands are highly overlapped, each sugar has a distinct spectral profile that differentiates it from others. The results show absorption zones dominated by two water bands at 3284 cm^{-1} (OH stretching) and 1641 cm^{-1} (OH deformation) and the spectra in the regions corresponding to sugars. Moreover, unlike

Table 1: Predominant of FTIR peaks for Maui Raws Turbinado brown sugar.

Wavenumber (cm^{-1})	976	1003	1111
A (absorbance) before reduction	0.0043	0.0041	0.0033
A (absorbance) after reduction	0.0041	0.0036	0.0031

Table 2: Predominant of FTIR peaks for Splenda.

Wavenumber (cm^{-1})	999	1005	1113
A (absorbance) before reduction	0.0041	0.0046	0.0032
A (absorbance) after reduction	0.0038	0.0038	0.0030

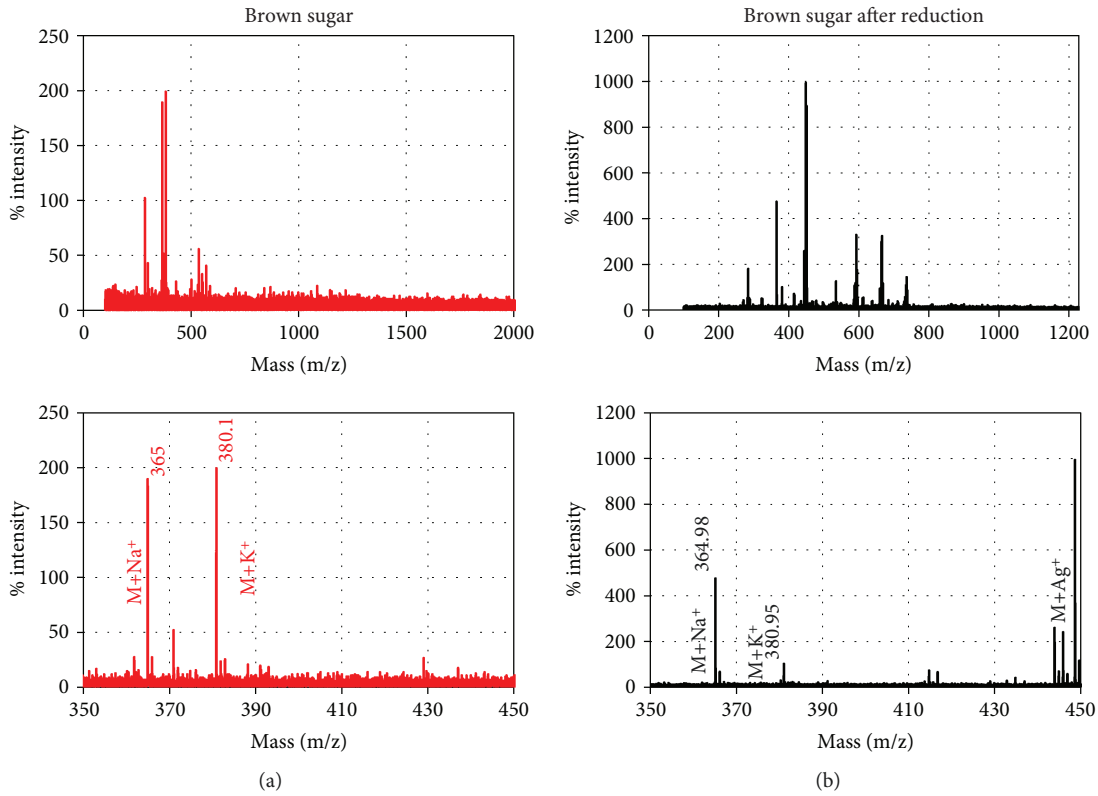

Figure 12: Mass spectra of 2 wt.% of brown sugar before and after reduction (10 mM $AgNO_3$, $T = 50^{\circ}C$, 2 h reaction time).

other simple molecules, sugars have endocyclic and exocyclic C-O bands, located at 995 cm^{-1} (exocyclic for sucrose) and around 1080 cm^{-1} (endocyclic for glucose and fructose). The peak in the range of 2330–2340 after reduction can be related to carbon dioxide (O=C=O stretching).

3.4. Mass Spectrometry (MS) Characterization of Reducing Agent before and after Reduction. Different types of ionization sources can be utilized for carbohydrate analysis, but the main one remains to be "matrix-assisted laser desorption ionization" (MALDI) that is a soft ionization technique that causes the formation of less unintended fragmentation during the ionization process (also called in-source fragmentation) [62]. Despite the fact that the MS technique has the capability to identify several compounds based on their mass spectrometric fragmentation patterns, the unambiguous identification of an individual sugar is complicated. This is because of the similarities in the MS fragmentation pattern observed for sugar compounds from the same group, for example, galactose and altrose or arabitol and xylitol [63]. As the exact ingredients of each artificial sweetener or sugar substitute are not known, the first step is to know the type and amounts of, for instance, monosaccharides that compose a particular structure of interest [62].

The mass spectrometry analyses were done on both brown sugar and Splenda before and after reduction. Figure 12 shows the mass spectra of brown sugar before and after reduction with the corresponding peaks. The mass spectrum of brown sugar before reduction shows sucrose plus sodium and sucrose plus potassium, which depicts the presence of sucrose with MW of 342.3 ((glucose with MW of 180.16) + (fructose with MW of 180.16) − (H_2O with MW of 18)). The mass spectrometry of brown sugar after reduction shows those but sucrose plus two isotopes of silver (^{107}Ag:^{109}Ag) with a 1 : 1 ratio as well. In the case of silver formation, the Ag cations are not unexpected, and whether or not sugar is around, this would result in the formation of $(M + Ag)^+$ ions. Separation of all AgNPs with the first step of centrifugation has been tried in order to have only the reducing agent after reduction, but there is the possibility of the presence of very tiny AgNPs that cannot be separated by centrifugation. The UV-vis data showed that sucrose by itself does not act as a reducing agent; therefore, something else in brown sugar, such as molasses, may be responsible for the reduction of silver ions.

Mass spectra of Splenda before and after reduction with corresponding peaks are shown in Figure 13. It is clear to see the equivalent of poly-glucose plus sodium in the range of 1000–1200 m/z but, in another area of the spectra (1200–3700 m/z), is obviously different numbers of the equivalent of poly-glucose, which has a net loss of one water (H_2O) molecule combining the glucose entities. Mass spectra of Splenda after reduction shows sugar modules plus two isotopes of silvers (^{107}Ag:^{109}Ag) with a 1 : 1 ratio.

These comparisons illustrate how these two reducing agents act differently in the reduction of silver ions to silver atoms, but more characterization such as nuclear magnetic resonance (NMR) and Raman is required to find out the exact differences and ability of each functional group as the reducing agent.

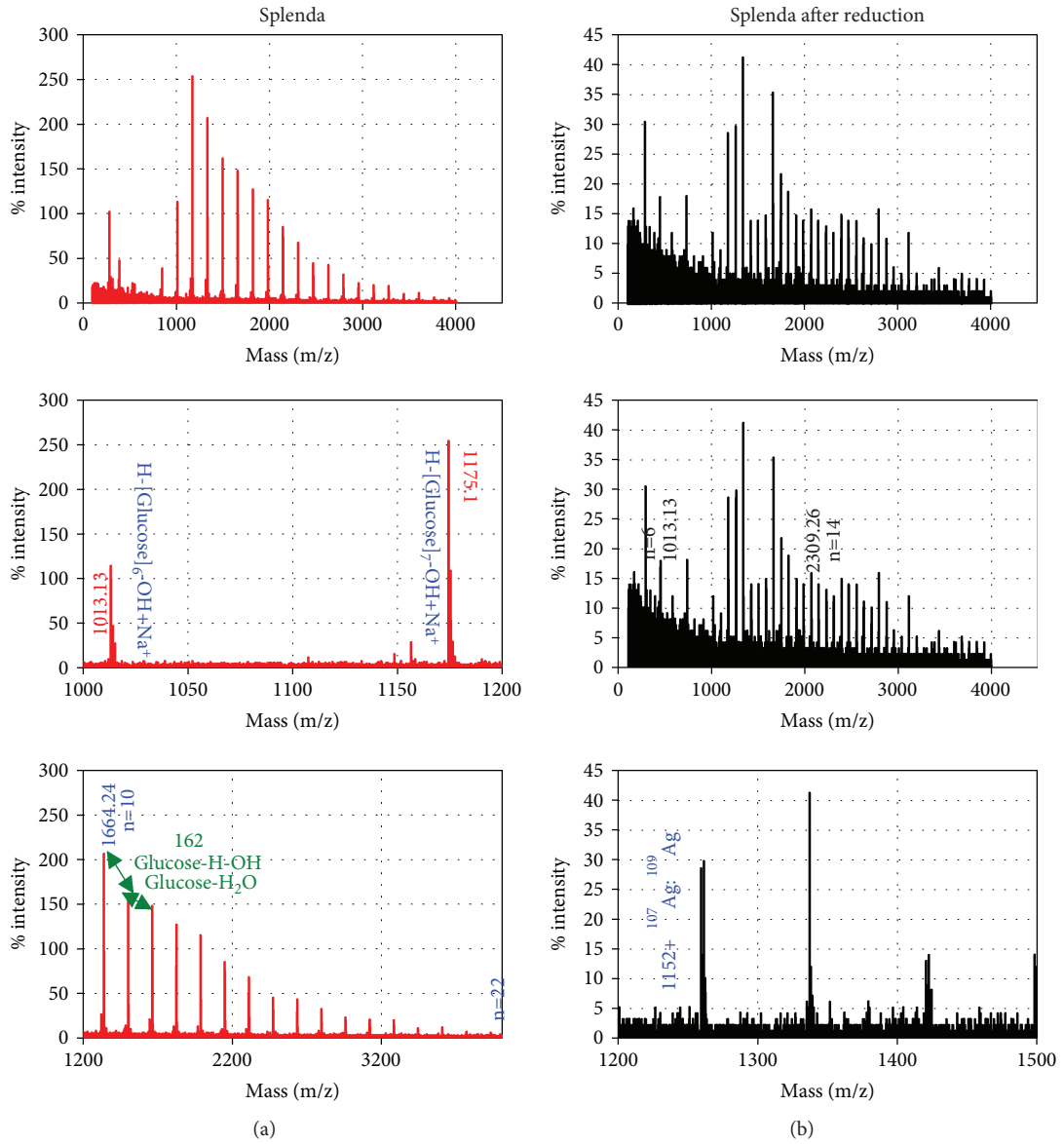

Figure 13: Mass spectra of 2 wt.% of Splenda before and after reduction (10 mM $AgNO_3$, $T = 50^{\circ}C$, 2 h reaction time).

3.5. Conclusion. In this study, AgNPs were synthesized by utilizing different sugars and artificial sweeteners as reducing agents in a green, eco and cost-effective, rapid, and sustainable manner. Different artificial sweeteners and sugar substitutes in different color packets that illustrate the different main ingredients showed different ability towards Ag ion reduction and AgNP formation. It was shown that among several artificial sweeteners and sugar substitutes with different packet colors, yellow packets containing sucralose and maltodextrin as the main ingredients could act as reducing agents even in the absence of NaOH. Further studies will also consider the reduction ability of other sugar substitutes (Sweet'n Low and Equal Original) with different packet colors such as pink and blue in the presence of NaOH.

In future studies, it is essential to optimize this process in terms of reaction conditions to maximize AgNP yield for large-scale industrial production. This is the first study in the synthesis of AgNPs using different commercially available artificial sweeteners. For the first time, it was shown that the Maui Raws Turbinado brown sugar can act as both a reducing agent and a capping agent to synthesize 1D Ag nanostructures even in the absence of a capping agent such as PVP. Future investigations will focus on the mechanisms and the functional groups that allow the production of 1D Ag nanostructures using this specific brown sugar.

The utilization of cheap, environmentally friendly, and renewable materials, such as artificial sweeteners and sugar substitutes, provides lots of advantages of ecofriendliness and biocompatibility for biomedical and pharmaceutical applications. Moreover, the simplicity and economic sustainability associated with the synthesis process make it amenable to the large-scale industrial production of AgNPs.

Data Availability

The datasets generated during the current study are available from the corresponding author on reasonable request.

Conflicts of Interest

The authors declare that they have no conflicts of interest.

Acknowledgments

This research was funded by the College of Engineering at Purdue University and received funding from Robert B. and Virginia V. Colvalt Professorship Endowment.

Supplementary Materials

Figure S1: UV-vis characterization during the synthesis of AgNPs (1 mM $AgNO_3$, 2 wt.% sugar substitutes or artificial sweeteners, $T = 25^{\circ}C$, 2 h reaction time). Figure S2: UV-vis characterization during the synthesis of AgNPs (1 mM $AgNO_3$, 1.6 mM PVP, 2 wt.% sugar substitutes or artificial sweeteners, $T = 50^{\circ}C$, 2 h reaction time). Figure S3: UV-vis characterization during the synthesis of AgNPs (10 mM $AgNO_3$, 16 mM PVP, 2 wt.% sugar substitutes or artificial sweeteners, $T = 50^{\circ}C$, 2 h reaction time). Figure S4: UV-vis characterization during the synthesis of AgNPs (1 mM $AgNO_3$, $T = 50^{\circ}C$, 2 h reaction time). Figure S5: pH measurement during the synthesis of AgNPs in the presence of NaOH (10 mM $AgNO_3$, $T = 50^{\circ}C$, 2 h reaction time). 20. Figure S6: pH measurement during the synthesis of AgNPs utilizing NaOH as a reducing agent (10 mM $AgNO_3$, $T = 50^{\circ}C$, 2 h reaction time). Figure S7: TEM images of the synthesized AgNPs utilizing Maui Raws Turbinado brown sugar as a reducing agent (1 mM $AgNO_3$, $T = 50^{\circ}C$, 2 h reaction time). Figure S8: TEM images of the synthesized AgNPs utilizing Splenda (yellow packet) as a reducing agent (1 mM $AgNO_3$, $T = 50^{\circ}C$, 2 h reaction time). Figure S9: TEM images of the synthesized AgNPs utilizing sucralose (A) and saccharin (B). Table S1: UV-vis result summary. *(Supplementary Materials)*

References

[1] A. K. Ojha, S. Forster, S. Kumar, S. Vats, S. Negi, and I. Fischer, "Synthesis of well-dispersed silver nanorods of different aspect ratios and their antimicrobial properties against gram positive and negative bacterial strains," *Journal of Nanobiotechnology*, vol. 11, no. 1, p. 42, 2013.

[2] S. Iravani, "Green synthesis of metal nanoparticles using plants," *Green Chemistry*, vol. 13, no. 10, p. 2638, 2011.

[3] S. F. Adil, M. E. Assal, M. Khan, A. Al-Warthan, M. R. H. Siddiqui, and L. M. Liz-Marzan, "Biogenic synthesis of metallic nanoparticles and prospects toward green chemistry," *Dalton Transactions*, vol. 44, no. 21, pp. 9709–9717, 2015.

[4] S. P. Dubey, M. Lahtinen, and M. Sillanpaa, "Green synthesis and characterizations of silver and gold nanoparticles using leaf extract of Rosa rugosa," *Colloids and Surfaces A: Physicochemical and Engineering Aspects*, vol. 364, no. 1-3, pp. 34–41, 2010.

[5] M. Parveen, F. Ahmad, A. M. Malla, and S. Azaz, "Microwave-assisted green synthesis of silver nanoparticles from Fraxinus excelsior leaf extract and its antioxidant assay," *Applied Nanoscience*, vol. 6, no. 2, pp. 267–276, 2016.

[6] S. P. Chandran, M. Chaudhary, R. Pasricha, A. Ahmad, and M. Sastry, "Synthesis of gold nanotriangles and silver nanoparticles using aloe vera plant extract," *Biotechnology Progress*, vol. 22, no. 2, pp. 577–583, 2006.

[7] H. R. Rajabi, H. Deris, and H. S. Faraji, "A facile and green biosynthesis of silver nanostructures by aqueous extract of Suaeda acuminata after microwave assisted extraction," *Nanochemistry Research*, vol. 1, no. 2, pp. 177–182, 2016.

[8] N. A. Zamanhuri, R. Alrozi, M. S. Osman, and M. A. M. Ariff, "Green synthesis and characterizations of silver and gold nanoparticles using pink guava waste extract (PGWE)," in *2012 IEEE Symposium on Humanities, Science and Engineering Research*, Kuala Lumpur, Malaysia, June 2012.

[9] P. Vishnukumar, S. Vivekanandhan, and S. Muthuramkumar, "Plant-mediated biogenic synthesis of palladium nanoparticles: recent trends and emerging opportunities," *ChemBioEng Reviews*, vol. 4, no. 1, pp. 18–36, 2017.

[10] K. Jyoti and A. Singh, "Green synthesis of nanostructured silver particles and their catalytic application in dye degradation," *Journal of Genetic Engineering and Biotechnology*, vol. 14, no. 2, pp. 311–317, 2016.

[11] P. Dwivedi, S. S. Narvi, and R. P. Tewari, "Phytofabrication characterization and comparative analysis of Ag nanoparticles by diverse biochemicals from Elaeocarpus ganitrus Roxb., Terminalia arjuna Roxb., Pseudotsuga menzietii, Prosopis spicigera, Ficus religiosa, Ocimum sanctum, Curcuma longa," *Industrial Crops and Products*, vol. 54, pp. 22–31, 2014.

[12] W. Yang, L. Zhang, Y. Hu, Y. Zhong, H. B. Wu, and X. W. D. Lou, "Microwave-assisted synthesis of porous Ag2S–ag hybrid nanotubes with high visible-light photocatalytic activity," *Angewandte Chemie*, vol. 124, no. 46, pp. 11669–11672, 2012.

[13] J. Li, Y. Xie, Y. Zhong, and Y. Hu, "Facile synthesis of Z-scheme Ag_2CO_3/ag/AgBr ternary heterostructured nanorods with improved photostability and photoactivity," *Journal of Materials Chemistry A*, vol. 3, no. 10, pp. 5474–5481, 2015.

[14] R. Qiao, M. Mao, E. Hu, Y. Zhong, J. Ning, and Y. Hu, "Facile formation of mesoporous $BiVO_4$/ag/AgCl heterostructured microspheres with enhanced visible-light photoactivity," *Inorganic Chemistry*, vol. 54, no. 18, pp. 9033–9039, 2015.

[15] W. Yang, J. Li, Y. Zhong, H. Qian, Z. Li, and Y. Hu, "Facile Cl^--mediated hydrothermal synthesis of large-scale Ag nanowires from AgCl hydrosol," *CrystEngComm*, vol. 15, no. 14, 2013.

[16] Z. Hosseinidoust, M. Basnet, T. G. M. van de Ven, and N. Tufenkji, "One-pot green synthesis of anisotropic silver nanoparticles," *Environmental Science: Nano*, vol. 3, no. 6, pp. 1259–1264, 2016.

[17] I. Hussain, N. B. Singh, A. Singh, H. Singh, and S. C. Singh, "Green synthesis of nanoparticles and its potential application," *Biotechnology Letters*, vol. 38, no. 4, pp. 545–560, 2016.

[18] M. M. Kemp, A. Kumar, S. Mousa et al., "Synthesis of gold and silver nanoparticles stabilized with glycosaminoglycans having distinctive biological activities," *Biomacromolecules*, vol. 10, no. 3, pp. 589–595, 2009.

[19] S. K. Batabyal, C. Basu, A. R. Das, and G. S. Sanyal, "Green chemical synthesis of silver nanowires and microfibers using

starch," *Journal of Biobased Materials and Bioenergy*, vol. 1, pp. 143–147, 2007.

[20] M. Naghdi, M. Taheran, S. K. Brar, M. Verma, R. Y. Surampalli, and J. R. Valero, "Green and energy-efficient methods for the production of metallic nanoparticles," *Beilstein Journal of Nanotechnology*, vol. 6, pp. 2354–2376, 2015.

[21] E. Abbasi, M. Milani, S. F. Aval et al., "Silver nanoparticles: synthesis methods, bio-applications and properties," *Critical Reviews in Microbiology*, vol. 42, no. 2, pp. 1–8, 2016.

[22] R. M. Ammal and G. Vijistella Bai, "Green synthesis of silver nanostructures against human cancer cell lines and certain pathogens," *International Journal of Pharmaceutical, Chemical & Biological Sciences*, vol. 4, no. 1, pp. 101–111, 2014.

[23] B. M. M. May and O. S. Oluwafemi, "Sugar-reduced gelatin-capped silver nanoparticles with high selectivity for colorimetric sensing of Hg2+ and Fe2+ Ions in the midst of other metal ions in aqueous solutions," *International Journal of Electrochemical Science*, vol. 11, pp. 8096–8108, 2016.

[24] S. Lebaschi, M. Hekmati, and H. Veisi, "Green synthesis of palladium nanoparticles mediated by black tea leaves (Camellia sinensis) extract: catalytic activity in the reduction of 4-nitrophenol and Suzuki-Miyaura coupling reaction under ligand-free conditions," *Journal of Colloid and Interface Science*, vol. 485, pp. 223–231, 2017.

[25] R. Geethalakshmi and D. V. L. Sarada, "Characterization and antimicrobial activity of gold and silver nanoparticles synthesized using saponin isolated from Trianthema decandra L," *Industrial Crops and Products*, vol. 51, pp. 107–115, 2013.

[26] A. A. Zahir and A. A. Rahuman, "Evaluation of different extracts and synthesised silver nanoparticles from leaves of Euphorbia prostrata against Haemaphysalis bispinosa and Hippobosca maculata," *Veterinary Parasitology*, vol. 187, no. 3-4, pp. 511–520, 2012.

[27] U. Y. Qazi and R. Javaid, "A review on metal nanostructures: preparation methods and their potential applications," *Advances in Nanoparticles*, vol. 5, no. 1, pp. 27–43, 2016.

[28] A. Dumas and P. Couvreur, "Palladium: a future key player in the nanomedical field?," *Chemical Science*, vol. 6, no. 4, pp. 2153–2157, 2015.

[29] J. Y. Choen and W. H. Park, "Green synthesis of silver nanoparticles stabilized with mussel-inspired protein and colorimetric sensing of lead(II) and copper(II) ions," *International Journal of Molecular Sciences*, vol. 17, no. 12, p. 2006, 2016.

[30] S. Basu, P. Maji, and J. Ganguly, "Rapid green synthesis of silver nanoparticles by aqueous extract of seeds of Nyctanthes arbor-tristis," *Applied Nanoscience*, vol. 6, no. 1, pp. 1–5, 2016.

[31] V. Kumar, D. Bano, S. Mohan, D. K. Singh, and S. H. Hasan, "Sunlight-induced green synthesis of silver nanoparticles using aqueous leaf extract of Polyalthia longifolia and its antioxidant activity," *Materials Letters*, vol. 181, pp. 371–377, 2016.

[32] S. Chairam and E. Somsook, "Facile, versatile and green synthesis of silver nanoparticles by mung bean starch and their catalytic activity in the reduction of 4-nitrophenol," *Chiang Mai Journal of Science*, vol. 43, no. 3, pp. 609–619, 2016.

[33] K. Jia, H. Shou, P. Wang, X. Zhou, and X. Liu, "Controlled synthesis of silver nanostructures stabilized by fluorescent polyarylene ether nitrile," *Applied Surface Science*, vol. 377, pp. 180–183, 2016.

[34] B. Khodashenas and H. R. Ghorbani, "Synthesis of silver nanoparticles with different shapes," *Arabian Journal of Chemistry*, 2015.

[35] M. Zargar, K. Shameli, G. R. Najafi, and F. Farahani, "Plant mediated green biosynthesis of silver nanoparticles using Vitex negundo L. extract," *Journal of Industrial and Engineering Chemistry*, vol. 20, no. 6, pp. 4169–4175, 2014.

[36] M. Noroozi, A. Zakaria, M. M. Moksin, Z. A. Wahab, and A. Abedini, "Green formation of spherical and dendritic silver nanostructures under microwave irradiation without reducing agent," *International Journal of Molecular Sciences*, vol. 13, no. 7, pp. 8086–8096, 2012.

[37] R. B. Devi, N. H. K. Sarma, W. Radhapiyari, and C. Brajakishor, "Green synthesis, characterization and antimicrobial properties of silver nanowires by aqueous leaf extract of piper betle," *International Journal of Pharmaceutical Sciences Review and Research*, vol. 26, pp. 309–313, 2014.

[38] A. N. Mishra, S. Bhadauria, M. S. Gaur, R. Pasricha, and B. S. Kushwah, "Synthesis of gold nanoparticles by leaves of zero-calorie sweetener herb (Stevia rebaudiana) and their nanoscopic characterization by spectroscopy and microscopy," *International Journal of Green Nanotechnology: Physics and Chemistry*, vol. 1, no. 2, pp. P118–P124, 2010.

[39] A. K. Shukla and S. Iravani, "Green synthesis and spectroscopic characterization of nanoparticles," in Springer International Publishing, Switzerland, 2016, Sustainable Agriculture Reviews 20.

[40] S. Mohan, O. S. Oluwafemi, S. C. George et al., "Completely green synthesis of dextrose reduced silver nanoparticles, its antimicrobial and sensing properties," *Carbohydrate Polymers*, vol. 106, pp. 469–474, 2014.

[41] D. Philip, "Honey mediated green synthesis of silver nanoparticles," *Spectrochimica Acta Part A: Molecular and Biomolecular Spectroscopy*, vol. 75, no. 3, pp. 1078–1081, 2010.

[42] D. Yu and V. W. W. Yam, "Hydrothermal-induced assembly of colloidal silver spheres into various nanoparticles on the basis of HTAB-modified silver mirror reaction," *The Journal of Physical Chemistry B*, vol. 109, no. 12, pp. 5497–5503, 2005.

[43] A. Mao, X. Jin, X. Gu, X. Wei, and G. Yang, "Rapid, green synthesis and surface-enhanced Raman scattering effect of single-crystal silver nanocubes," *Journal of Molecular Structure*, vol. 1021, pp. 158–161, 2012.

[44] S. M. Meshram, S. R. Bonde, I. R. Gupta, A. K. Gade, and M. K. Rai, "Green synthesis of silver nanoparticles using white sugar," *IET Nanobiotechnology*, vol. 7, no. 1, pp. 28–32, 2013.

[45] P. Nalawade, P. Mukherjee, and S. Kapoor, "Biosynthesis, characterization and antibacterial studies of silver nanoparticles using pods extract of Acacia auriculiformis," *Spectrochimica Acta Part A: Molecular and Biomolecular Spectroscopy*, vol. 129, pp. 121–124, 2014.

[46] M. Gnanadesigan, M. Anand, S. Ravikumar et al., "Biosynthesis of silver nanoparticles by using mangrove plant extract and their potential mosquito larvicidal property," *Asian Pacific Journal of Tropical Medicine*, vol. 4, no. 10, pp. 799–803, 2011.

[47] I. Calinescu, M. Patrascu, A. I. Gavrila, A. Trifan, and C. Boscornea, "Synthesis and characterization of silver nanoparticles in the presence of PVA and tannic acid," *UPB Scientific Bulletin, Series B*, vol. 73, no. 4, pp. 3–10, 2011.

[48] S. Rajeshkumar, "Synthesis of silver nanoparticles using fresh bark of Pongamia pinnata and characterization of its

antibacterial activity against gram positive and gram negative pathogens," *Resource-Efficient Technologies*, vol. 2, no. 1, pp. 30–35, 2016.

[49] M. H. El-Rafie, H. B. Ahmed, and M. K. Zahran, "Facile precursor for synthesis of silver nanoparticles using alkali treated maize starch," *International Scholarly Research Notices*, vol. 2014, Article ID 702396, 12 pages, 2014.

[50] S. Azizi, F. Namvar, M. Mahdavi, M. B. Ahmad, and R. Mohamad, "Biosynthesis of silver nanoparticles using brown marine macroalga, Sargassum muticum aqueous extract," *Materials*, vol. 6, no. 12, pp. 5942–5950, 2013.

[51] T. P. Devi, S. Kulanthaivel, D. Kamil, J. L. Borah, N. Prabhakaran, and N. Srinivasa, "Biosynthesis of silver nanoparticles from Trichoderma species," *Indian Journal of Experimental Biology*, vol. 51, no. 7, pp. 543–547, 2013.

[52] A. D. Pomogailo and G. I. Dzhardimalieva, "Reduction of metal ions in polymer matrices as a condensation method of nanocomposite synthesis," in *Nanostructured Materials Preparation via Condensation Ways*, Springer, Dordrecht, 2014.

[53] S. Hemmati, D. P. Barkey, N. Gupta, and R. Banfield, "Synthesis and characterization of silver nanowire suspensions for printable conductive media," *ECS Journal of Solid State Science and Technology*, vol. 4, no. 4, pp. P3075–P3079, 2015.

[54] S. Hemmati and D. P. Barkey, "Parametric study, sensitivity analysis, and optimization of polyol synthesis of silver nanowires," *ECS Journal of Solid State Science and Technology*, vol. 6, no. 4, pp. P132–P137, 2017.

[55] M. Teodorescu and M. Bercea, "Poly(vinylpyrrolidone) – a versatile polymer for biomedical and beyond medical applications," *Polymer-Plastics Technology and Engineering*, vol. 54, no. 9, pp. 923–943, 2015.

[56] S. Hemmati, D. P. Barkey, L. Eggleston, B. Zukas, N. Gupta, and M. Harris, "Silver nanowire synthesis in a continuous millifluidic reactor," *ECS Journal of Solid State Science and Technology*, vol. 6, no. 4, pp. P144–P149, 2017.

[57] E. Filippo, A. Serra, A. Buccolieri, and D. Manno, "Green synthesis of silver nanoparticles with sucrose and maltose: morphological and structural characterization," *Journal of Non-Crystalline Solids*, vol. 356, no. 6-8, pp. 344–350, 2010.

[58] G. Suresh, P. H. Gunasekar, D. Kokila et al., "Green synthesis of silver nanoparticles using Delphinium denudatum root extract exhibits antibacterial and mosquito larvicidal activities," *Spectrochimica Acta Part A: Molecular and Biomolecular Spectroscopy*, vol. 127, pp. 61–66, 2014.

[59] V. Kathiravan, S. Ravi, and S. Ashokkumar, "Synthesis of silver nanoparticles from Melia dubia leaf extract and their in vitro anticancer activity," *Spectrochimica Acta Part A: Molecular and Biomolecular Spectroscopy*, vol. 130, pp. 116–121, 2014.

[60] D. A. Kumar, V. Palanichamy, and S. M. Roopan, "Green synthesis of silver nanoparticles using Alternanthera dentata leaf extract at room temperature and their antimicrobial activity," *Spectrochimica Acta Part A: Molecular and Biomolecular Spectroscopy*, vol. 127, pp. 168–171, 2014.

[61] M. Khan, M. Khan, S. F. Adil et al., "Green synthesis of silver nanoparticles mediated by Pulicaria glutinosa extract," *International Journal of Nanomedicine*, vol. 8, pp. 1507–1516, 2013.

[62] G. L. Sassaki and L. M. de Souza, "Mass spectrometry strategies for structural analysis of carbohydrates and glycoconjugates," in *Tandem Mass Spectrometry-Molecular Characterization*, INTECH, 2013.

[63] P. M. Medeiros and B. R. T. Simoneit, "Analysis of sugars in environmental samples by gas chromatography–mass spectrometry," *Journal of Chromatography A*, vol. 1141, no. 2, pp. 271–278, 2007.